International Journal of Engineering Sciences Paradigms and Researches (IJESPR)
(Vol. 36, Issue 01) and (Publishing Month: November 2016)
(An Indexed, Referred and Impact Factor Journal)
ISSN: 2319-6564
www.ijesonline.com

Optimization of Organic Rankine Cycle (ORC) system driven by solar energy with sensible thermal energy storage

Bidyuta Ranjan Rout[1] and Pradyut Kumar Swain[2]

[1]Aryan Institute of Engineering & Technology, Bhubaneswar, Odisha

[2]NM Institute of Engineering and Technology, Bhubaneswar, Odisha

A R T I C L E I N F O

Keywords:
Solar energy
Organic Rankine Cycle
Energy storage
Optimal operation

A B S T R A C T

The best design and operation of an Organic Rankine Cycle (ORC) system powered by solar energy are studied in this study. The intermittency of solar energy is overcome by a two-tank sensible thermal energy storage system. This paper develops a simulation-based optimization methodology. The ORC's process simulation is done in Aspen HYSYS, while the energy storage system and parabolic trough collector mathematical models are created in MATLAB. The system's optimal design, including the hot tank temperature, cold tank temperature, HTF mass flowrate, and ORC operating conditions, is established simultaneously using simulation-based optimization.

1. Introduction

Pressing climate change along with technological advancements has spurred the growth of renewable energy installations in the last decade [1]. The greenhouse gas emissions from conventional power generation are receiving increasing attention. Environmentally friendly and energy-efficient power generation technologies represent a general trend in the future energy market. Solar energy utilization is a promising way to generate electricity because of its abundance and availability [2]. Electricity production from solar energy has been proven to be a viable option for green energy production. Among various solar energy technologies, concentrated solar power (CSP) is attractive due to its high efficiency, low operating cost, and flexible scale-up potential [3].

Furthermore, there are different CSP technologies such as parabolic trough collectors (PTC), linear Fresnel reflectors (LFR), solar power towers (SPT), and parabolic dish reflectors [4]. The PTC technology is one of the most advanced solar thermal energy technologies with considerable operational experience and has the advantage of low installation cost compared to other technologies. PTCs can effectively produce heat at temperatures between 50 °C and 400 °C [4]. Several different potential power cycles can convert heat into power. The most versatile and efficient power cycle below 400 °C is the Organic Rankine Cycle (ORC) [5], which is widely used for low-temperature waste heat recovery in the industry [6]. Although the conventional steam Rankine cycle dominates in terms of efficiency when utilizing heat sources at temperatures of 400 °C or higher, these temperatures are out of reach for many conventional PTC technologies. In addition, the ORC is more

Nomenclature

Abbreviation

CSP	concentrated solar power
CPC	compound parabolic collector
DNI	direct normal irradiance
FPC	flat plate collector
HTF	heat transfer fluid
LFR	linear Fresnel reflector
LNG	liquefied natural gas
ORC	Organic Rankine Cycle
PDC	parabolic dish collector
PTC	parabolic trough collector

Variables and parameters

A_c	solar collector area
C_p	specific heat capacity
G_b	beam irradiation
P	pressure
Q	heat load
T	temperature
h	specific enthalpy
m_c	mass flowrate of HTF through the solar collector
m_{HTF}	mass flowrate of HTF through the ORC evaporator
m_{orc}	mass flowrate of the organic working fluid
W	work
η	efficiency

Subscript and Superscript

c	critical property
cold	cold storage tank
eva	evaporation
hot	hot storage tank
inlet	inlet stream
net	net power output
1,2,3…	different state points in the system
s	saturation state
	turbine

compact and less costly compared with the conventional steam Rankine cycle power plant [7].

A transcritical CO_2 cycle is also an alternative for solar energy utilization if a low temperature heat sink is available. Mehrpooya and Sharifzadeh [8] proposed a novel oxy-fuel transcritical Rankine cycle with carbon capture for the simultaneous utilization of solar energy and liquefied natural gas (LNG) cold energy. A thermal energy storage tank was adopted to overcome the intermittency of solar energy. Ahmadi et al. [9] performed a techno-economic analysis and multi-objective optimization of a transcritical CO_2 power cycle driven by solar energy and LNG cold energy. A heat storage tank and an auxiliary heater are configured in their system as well. It is obvious that energy storage is necessary for solar energy utilization by means of power cycles. However, without a perfect heat sink like LNG, an Organic Rankine Cycle is more suitable for solar energy utilization. Cocco and Serra [10] compared the solar-powered ORC system with a two-tank direct energy storage system and a thermocline energy storage system, and concluded that the two-tank direct energy storage system shows slightly higher efficiency. Wang et al. [11] investigated the off-design performance of a solar-powered ORC, where only one tank is considered. To avoid off-design operation of the ORC system, Yang et al. [12] proposed a novel operating mode of the ORC system with a two-tank energy storage system under nominal design conditions. This novel operating mode can maintain high efficiency of the ORC system with stable power output. However, process optimization and optimal operation of the energy storage system were not thoroughly addressed in their study. Table 1 summarizes the key contributions and characteristics of relevant previous studies and this study.

Table 1
Summary of key characteristics of the previous studies and this study.

References	Solar collector	Power cycle	Energy storage	Stable power output	Optimization
[8]	CPC	CO_2 Cycle	One Tank	Yes	No
[9]	FPC	CO_2 Cycle	One Tank	No	Yes
[10]	LFC	ORC	One/Two Tanks	Yes	Partially done
[11]	CPC	ORC	One Tank	No	No
[12]	PTC	ORC	Two Tanks	Yes	No
This study	PTC	ORC	Two Tanks	Yes	Yes

The main objective of this study is to determine the optimal design and optimal operating strategy for the two-tank storage solar energy driven ORC system proposed by Yang et al. [12] and carry out a thorough performance analysis under different assumptions. The main contributions of this study are the following: (1) A simulation-based optimization framework is developed to optimize the performance of the solar driven ORC system with round-the-clock electricity generation. (2) The impacts on the system performance of (i) system configuration (basic ORC vs. recuperative ORC), (ii) power cycle type (subcritical vs. supercritical), and (iii) working fluids are investigated thoroughly. The rest of this paper is organized as follows: Section 2 presents the detailed description of the solar energy driven ORC power plant with energy storage. The mathematical model and process simulation model along with the optimization algorithm used in this study are presented in Section 3. The optimal results and the main findings are analyzed in Section 4. Section 5 summarizes the conclusions of this study.

2. Process description

The peak hours of solar irradiation are usually in hours of low electricity demand in the grid. Without energy storage technology, the solar power plant has to be operated at off-design conditions most of the time, which leads to the quite low thermal efficiency of the ORC and low overall system efficiency. Therefore, thermal energy storage (TES) is normally configured to overcome this challenge, and thus the profit of the solar energy power plant can be improved [13]. With the TES system, the solar power plant can not only generate electricity round-the-clock but also operate at nominal design conditions to maintain high efficiency. TES technology, acting like a buffer between the solar collector and the power generating unit, allows for flexibility of the power system. The periods with high solar intensity do not correspond to the periods with high power demand. Thus, the energy can be stored in periods with high solar intensity and low power demand, and be released in periods with low solar intensity and high power demand [3]. TES systems can be classified into sensible heat, latent heat and thermochemical energy storage technologies [14], while TES systems can also be classified as direct and indirect based on the heat transfer fluid and the storage medium [15]. The two-tank energy storage system proposed by Yang et al. [12] is shown in Fig. 1. This system has been proven to be an efficient system configuration for solar energy

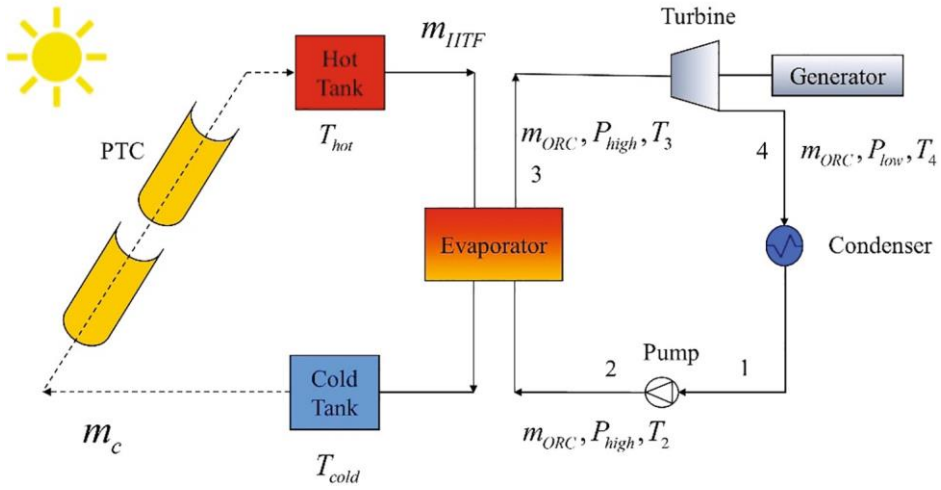

Fig. 1. Flowsheet of the basic ORC system with two-tank energy storage [12].

utilization with stable power output. In our study, the two-tank energy storage system, which can also be categorized as a direct and sensible thermal energy storage, is chosen as the TES system.

In this study, the integrated system consists of a solar energy collecting sub-system, thermal energy storage sub-system, and an ORC power generation sub-system. The parabolic trough collector (PTC) was selected as the solar collector as it can heat the heat transfer fluid (HTF) to relatively high temperatures with good efficiency, and this technology has reached the highest level of commercial maturity. PTC systems account for the largest share of the current concentrated solar power market compared with other technologies [16]. As shown by the dashed lines in Fig. 1, by adjusting the mass flowrate of the HTF through the solar collector (m_c), the HTF can be heated to a constant temperature even under varying solar insolation. The HTF can be released at a constant mass flowrate to the evaporator, where it delivers heat to the ORC sub-system; thus, the ORC can always operate stable at nominal design conditions. During solar peak hours, the HTF travels through the PTC from the cold tank at a high flowrate and then is stored in the hot tank. Stable operation of the system can avoid a drastic decrease of system efficiency during unstable operation, as shown in the work of Wang et al. [11]. The solid lines in Figs. 1 and 2 are meant to indicate that the flowrates of these streams are constant, while the dashed lines mean that the flowrate of such streams varies with the insolation. The pumps to circulate the HTF between the hot tank and the cold tank are omitted because their work requirements are negligible compared to the power output of the ORC sub-system.

The ORC sub-system consists of a pump, an evaporator, a turbine and a condenser as shown in Fig. 1. The organic working fluid is pumped from condensation pressure to evaporation pressure (process 1 → 2). After pumping, the organic working fluid is vaporized and superheated in the evaporator (process 2 → 3). Next, the high temperature and high pressure vapor is expanded through the turbine to generate power (process 3 → 4). Finally, the working fluid is condensed in the condenser (process 4 → 1). To improve the thermal efficiency of the ORC sub-system, a recuperator can be configured between the turbine outlet stream and the pump outlet stream to recover part of the condensation heat of the organic working fluid. Fig. 2 illustrates the layout of the integrated system with a recuperator.

With this configuration, the HTF from the hot tank to the cold tank can be maintained at constant flowrate and temperature, while the HTF from the cold tank to the hot tank varies with the insolation. Both the constant flowrate (m_{HTF}) and the variable flowrate (m_c) determine how much solar energy can be collected from the PTC and the efficiency of the ORC. In addition, the temperatures of the hot and cold tanks are critical for the integrated system for the following reasons: Both temperatures exert a great influence on the thermal efficiency of the ORC sub-system. The higher the hot tank temperature, the higher the thermal efficiency of the ORC sub-system. However, the temperature of the hot tank cannot be very high since the efficiency of the PTC will degrade at higher temperatures, which means less heat can be absorbed by the solar

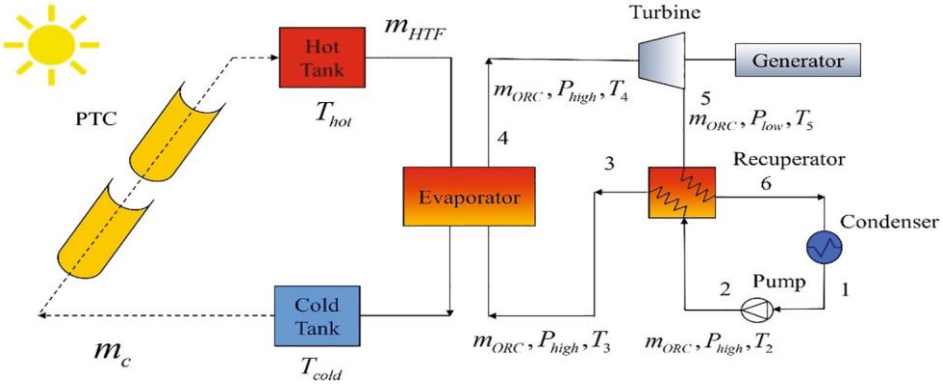

Fig. 2. Flowsheet of the recuperative ORC system with two-tank energy storage [12].

collector. Therefore, there is a trade-off between the PTC efficiency and the ORC efficiency. Moreover, the operating conditions of the ORC sub-system affect the HTF inlet temperature to the cold tank, and thus influences the PTC sub-system. It is obvious that the HTF is connecting the PTC, the thermal energy storage and the ORC sub-systems. The flowrate of the HTF, the target temperatures of hot and cold tanks, and the ORC operating conditions should be determined simultaneously to maximize the overall system efficiency of the solar energy power plant. The objective of this study is to determine the optimal design and operation of the integrated solar energy driven power plant, namely the optimal operating conditions of the ORC sub-system, the optimal design of the energy storage system, and the optimal operation of the PTC.

3. Modeling and optimization

To determine the optimal operation of the integrated solar-based power plant, Yang et al. [12] proposed a methodology for the optimal configuration of the system. The HTF inlet temperature to the evapo- rator is fixed at discrete values from 225 to 375 °C with 25 °C in- crements. For each HTF inlet temperature, an iterative procedure is performed to locate the optimal operating conditions of the integrated system. A large number of iterations is needed, and the process is tedious. Also, the optimal operating condition of the ORC system is determined under given HTF inlet temperatures, which means that the operating conditions of the ORC sub-system and the HTF inlet temper-ature are not optimized simultaneously. To address this shortcoming in their study, the HTF inlet temperature, the operating conditions of the ORC, and the optimal control of the energy storage system are optimized simultaneously in this work. An integrated model is developed in Matlab and Aspen HYSYS, which is a widely used process simulator, to obtain the optimal process design and control strategy of the solar energy driven ORC power plant. The thermal energy storage sub-system and the PTC sub-system are modeled in Matlab, while the ORC sub-system is simulated in Aspen HYSYS. The modeling of each sub-system is presented in the following.

The time horizon in this study is assumed to be one day as done by Yang et al. [12]. The direct normal irradiance (DNI) is divided into 24 time-intervals for one day. The irradiation and ambient temperature are assumed to be constant for each time-interval. The available energy from the sun in each time interval, Q_s, can be calculated by Eq. (1).

$$Q_s = A_c \cdot G_b \tag{1}$$

where A_c is the aperture area of the collector and G_b is the beam irradiation or the DNI.

The efficiency of the collector can be defined by Eq. (2).

$$\eta_c = \frac{Q_c}{Q_s} \tag{2}$$

where Q_c is the energy absorbed by the HTF in the collector.

The PTC chosen for modeling purposes in this study is the commercially available EuroTrough ET-150. This model was found to be both economical and effective for similar system layouts by Tzivanidis et al. [13]. The efficiency of the collector is given by Eq. (3), as suggested by Blanco et al. [17].

$$\eta_c = 0.75 - 0.000045\Delta T - 0.039\frac{\Delta T}{G_b} - 0.0003G_b\left(\frac{\Delta T}{G_b}\right)^2 \tag{3}$$

where G_b is the beam irradiation and ΔT is the difference between ambient temperature and mean temperature in the solar collector, as shown in Eq. (4) [17].

$$\Delta T = (T_{hot} + T_{cold})/2 - T_{amb} \tag{4}$$

where T_{amb} is the ambient temperature, which also has an impact on the system.

Given the temperatures of the HTF at the inlet and outlet of the collector and the mass flowrate through the collector, the heat absorbed by the HTF in the solar collector can be calculated by Eq. (5).

$$Q_c = m_c \cdot C_p^{HTF} \cdot (T_{hot} - T_{cold}) \tag{5}$$

where T_{hot} and T_{cold} are the temperatures of the hot and cold tanks, and C_p^{HTF} is the specific heat capacity of the HTF. Synthetic organic thermal oils are commonly used as the HTF in parabolic trough collectors. A mixture of Diphenyl Oxide and Biphenyl, with mass fractions of 73.5% and 26.5% respectively, is chosen as the HTF because the mixture can be used for temperatures up to 400 °C [18].

To determine the mass flowrate of the HTF, the specific heat capacity should be given. However, the specific heat capacity of the thermal oil mixture is unknown, and it is a function of temperature. Therefore, the specific heat capacities under different temperatures are retrieved from multiple simulations in Aspen HYSYS. Based on the simulation results, the specific heat capacity of the HTF is regressed as a function of tem- perature and shown in Eq. (6).

$$C_p^{HTF} = 3.3811 \cdot T + 1509.7 \tag{6}$$

Then the mass flowrate of the thermal oil to the ORC sub-system can be calculated by Eq. (7).

$$m_{HTF} = \frac{\sum_{i=1}^{24} m(i)_c}{24} \tag{7}$$

where i denotes the time intervals, which are assumed to be 24 in this study.

The evaporator of the ORC sub-system connects the energy storage system with the ORC sub-system. The energy balance between the organic working fluid in the ORC and the HTF in the solar energy storage system can be expressed by Eq. (8).

$$m_{HTF} \cdot C_p^{HTF} \cdot (T_{hot} - T_{cold}) = m_{ORC} \cdot (h_3 - h_2) \tag{8}$$

where m_{ORC} denotes the mass flowrate of the organic working fluid in the ORC system, and h_2 and h_3 are the specific enthalpies of the working fluid at state points 2 and 3 respectively, as shown in Fig. 1. The values of these parameters can be obtained from the Aspen HYSYS simulator. Aspen HYSYS is interfaced with Matlab with the help of ActXserver.

For the recuperative ORC system, E. (8) is modified to Eq. (9).

$$m_{HTF} \cdot C_p^{HTF} \cdot (T_{hot} - T_{cold}) = m_{ORC} \cdot (h_4 - h_3) \tag{9}$$

The ORC model is built in Aspen HYSYS, and the Peng-Robinson equation of state is chosen as the thermodynamic property method [19,20], which has been widely used to simulate ORC systems [21,22]. To be consistent with the work of Yang et al. [12], the same assumptions are adopted: (i) the solar irradiation and ambient temperature for each hour are assumed to be constant; (ii) pressure drop and heat loss for heat exchangers and storage tanks are neglected; (iii) condensation temperature of the ORC is assumed to be 50 °C; (iv) minimum heat transfer approach temperature is set to 20 °C; and (v) isentropic efficiencies of the turbine and pump are assumed to be 80% and 75% respectively.

The net power output of the ORC sub-system is calculated by Eq. (10).

$$W_{net} = W_{tur} - W_{pump} \tag{10}$$

The thermal efficiency of the ORC sub-system is defined by Eq. (11).

$$\eta_{ORC} = \frac{W_{net}}{m_{HTF} \cdot C_p^{HTF} \cdot (T_{hot} - T_{cold})} \tag{11}$$

The overall system efficiency is defined by Eq. (12).

$$\eta_{sys} = \frac{W_{net} \cdot 3600 \cdot 24}{A_b \sum_{i=1}^{24} G_b(i) \cdot 3600} \tag{12}$$

The objective function is the overall system efficiency, which is equivalent to maximizing the power output of the ORC system for a given area of solar collectors and DNI values.

Based on the ORC model in Aspen HYSYS, the collector model and thermal energy storage model in Matlab, the integrated system can be simulated and evaluated. The optimal operating conditions of the ORC sub-system, the optimal design of the energy storage system and the optimal operation of the solar collector system should be determined simultaneously by optimization. The particle swarm optimization (PSO) algorithm [23], inspired by the behavior of the flock and their ability to localize food as a group, is a computationally efficient algorithm and chosen for optimization in this study. The PSO algorithm is a meta-heuristic algorithm, which does not require gradient information and can escape from local optima. In addition, the PSO algorithm has the advantages of few tuning parameters and ease of implementation [24]. A population (called swarm) of potential solutions (called particles) moves around in the search space according to the particles positions and velocities [25]. The position of each particle in the PSO stands for a potential solution in the searching space. Each particle's movement is influenced by both its best-known position and the swarm's best-known position. This can speed up the process of locating the optimal solution [26]. This algorithm has been applied to many engineering problems and the effectiveness has been proven. Garg and Orosz [27] performed a thermo-economic optimization of a one-tank ORC system for waste heat and solar applications with the PSO algorithm. Liu et al. [28] applied the PSO algorithm to the multi-objective optimization of the fin-and-tube evaporator in a diesel engine ORC system. The PSO algorithm has been demonstrated to be robust in non-linear programming such as in heat exchanger network synthesis as well [29].

The PSO algorithm combining with Aspen HYSYS and Matlab capability is adopted to optimize the integrated ORC system in this

Table 2
Independent variables and their corresponding lower and upper bounds.

Variables	Unit	Lower bound	Upper bound
Hot tank temperature	°C	300	400
Cold tank temperature	°C	50	300
Mass flowrate of working fluid	kg/s	0	50
Evaporation pressure	bar	5	0.9·P_c
Cold tank temperature (recuperative ORC)	°C	100	300
Heat load of recuperator (recuperative ORC)	kW	50	500

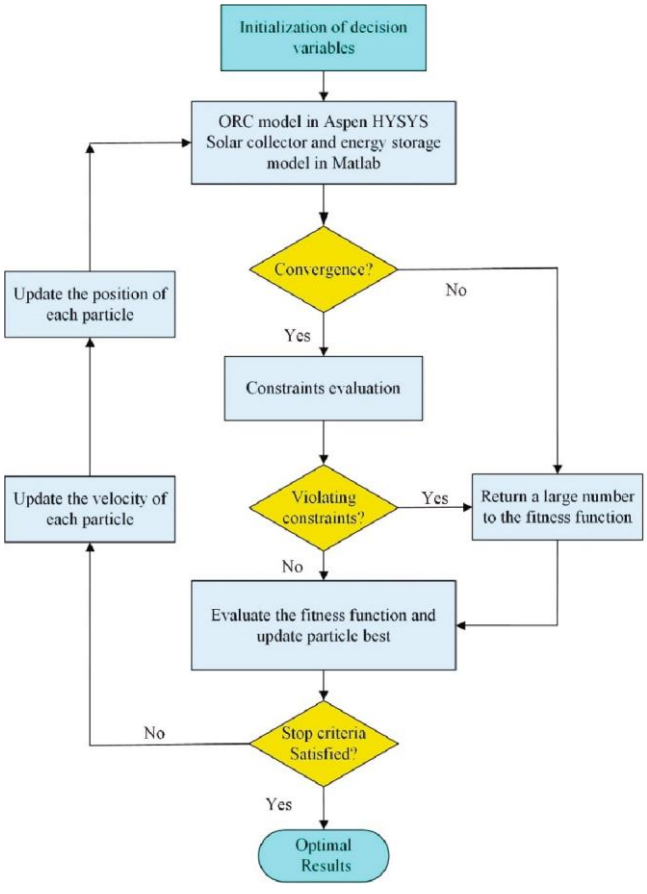

Fig. 3. Flowchart for the simulation-based PSO framework.

study. The flowchart of the simulation-based optimization framework is illustrated in Fig. 3. This framework takes advantage of the modeling capability of Aspen HYSYS and Matlab, and the optimization capability of the PSO algorithm. The PSO algorithm generates the initial values of the decision variables based on the given upper and lower bounds. After the initialization, the decision variables are sent to the ORC model in Aspen HYSYS and the solar collector and energy storage system model in Matlab. However, the initial values may be infeasible. If the models do not converge, a large enough number is returned to the fitness function to penalize the infeasibility of the initial values. This is inspired by the penalty method for constrained optimization algorithms. If the models converge, the algorithm proceeds to the next step, where the constraints are evaluated. If the constraints are violated, a larger number is returned to the fitness function. After checking the constraints, the fitness func- tion is evaluated for all the particles and the best particle can be ob- tained. Finally, the stop criteria of the algorithm are checked. If none of the criteria are satisfied, the algorithm proceeds to the next iteration, and the velocity and position of each particle will be updated based on information from the previous iterations. The optimal results are ob- tained when one of the stop criteria is satisfied.

Based on a degree freedom analysis for the basic ORC system, thefollowing 4 variables are chosen as the independent variables: (1) hottank temperature; (2) old tank temperature; (3) mass flowrate of theorganic working fluid of the ORC; and (4) evaporation pressure of theORC. For the recuperative ORC system, other than the above 4 degree offreedom, the heat load of the recuperator is chosen as the fifth inde-pendent variable since the heat exchanger heat load is easy to transferbetween Matlab and Aspen HYSYS compared with other parameters inthe model. The lower and upper bounds of the independent variables are listed in Table 2. It should be noted that the maximum evaporationpressure is set as 90% of the working fluid critical pressure. Thecondensation temperature, collectors' area, DNI, ambient temperature,turbine isentropic efficiency, pump isentropic efficiency, and motor ef-ficiency are given the same values as used in Yang et al.'s work [12].Since we will compare our results with Yang et al.'s work, the sameassumptions and parameters are used in this study. If other assumptionsare used, the results will be different, but the methodology is still valid.The following constraints are considered in this study: (1) minimum approach temperature of the recuperator and evaporator must be greater than 3 °C to avoid too large heat exchanger; (2) vapor fraction of the turbine inlet stream must be 100%; (3) vapor fraction of the turbine outlet stream must greater or equal to 95% to avoid blade erosion due to droplets formed at the outlet of the turbine; and (4) vapor fraction of the pump inlet stream must be 0 to guarantee normal operation of the pump. Finally, the optimization model can be formulated as follows:

$$\text{Maximize} \quad \eta_{sys} \qquad (\ )$$

$$\text{s.t.} \quad \text{Solar collector and thermal energy storage model in Equations 1 - 9} \qquad (\ )$$

$$\text{ORC model in Aspen HYSYSThe net power output in Equation 10}$$

$$\text{Heat exchanger approach temperature} \geqslant 3\text{K}$$

$$\text{Turbine inlet vapor fraction} = 1$$

$$\text{Turbine outlet vapor fraction} \geqslant 0.95$$

$$\text{Pump inlet stream vapor fraction} = 0$$

To make sure the search space is within the feasible region, a penalty function method is adopted to handle these constraints. Once a constraint is violated, a large penalty is added to the objective function to counteract the violation of the constraint, as shown in the flowchart in Fig. 3. The algorithm terminates when the maximum number of iterations or a specified tolerance is reached. The parameters of the PSO algorithm are set as follows: The maximum number of iterations is 100, the swarm size is 50, and the stop tolerance is set as 1e−5. The integrated optimization model is solved on a PC with 4 cores 2.8 GHz Intel i7 CUP and 32 GB of RAM running Windows 10.

4. Results and discussion

The DNI value and the corresponding ambient temperature profile are given and illustrated in Fig. 4. The DNI values taken from Yang et al. [12] represent a typical summer day in Yinchuan (38°28′59″N, 106°13′ 1″E), in the northwest part of China. Four working fluids (toluene, cyclohexane, hexamethyldisiloxane (HMDSO) and n-pentane) studied by Yang et al. [12] and two additional working fluids (benzene and n-hexane) are investigated in this study. The critical parameters of the investigated working fluids are listed in Table 3. Since the condensation temperature is assumed to be 50 °C, the saturation pressure at 50 °C indicates the condensation pressure. The saturation temperature at 1 bar is also an important parameter, because 1 bar is the minimum condensation pressure if vacuum operation is not allowed in the system. As shown in Table 3, n-pentane has the lowest condensation temperature at 1 bar, while other working fluids have considerably higher condensation temperatures. A high condensation temperature indicates a low thermal efficiency of the ORC.

Table 3
Critical properties for working fluids investigated in this study.

Working fluids	Chemical formula	T_c (°C)	P_c (bar)	T_s (°C) at 1 bar	P_s (bar) at 50 °C
Toluene	C_7H_8	318.8	41.23	111.7	0.12
Cyclohexane	C_2F_6	280.4	40.81	80.96	0.36
Hexamethyldisiloxane	O[Si(CH3)3]2	245.6	19.39	100.2	0.37
n-Pentane	C_5H_{12}-1	196.6	33.70	35.91	1.58
Benzene	C_6H_6	289.5	49.24	79.71	0.37
n-Hexane	C_6H_{14}-1	234.3	30.31	68.44	0.54

4.1. Basic ORC versus recuperative ORC

The optimal results of the basic ORC and the recuperative ORC are listed in Table 4. It is clear that for all investigated working fluids, the recuperative ORC can improve both the ORC thermal efficiency and the system efficiency significantly. For all of the working fluids investigated in this study, the improvement in ORC thermal efficiency lies in the range between 11.2 and 18.7% points, while the improvement in overall system efficiency is between 6.9 and 12% points. Toluene has the maximum power output for both basic and recuperative ORCs. The ORC thermal efficiency is improved from 24.3% to 36.3% with toluene as the working fluid. The overall system efficiency is improved from 17.4% to 24.8%. This shows that the recuperator can improve ORC thermal efficiency and overall system efficiency substantially. For the basic ORC, toluene and benzene perform much better than the other working fluids studied, while the superiority becomes marginal in the recuperative ORC. Hexamethyldisiloxane achieves the largest improvement when using recuperative ORC (18.7 and 12.0% points for ORC thermal efficiency and overall system efficiency respectively). For ORC applications in waste heat recovery, the recuperator is not always beneficial [30]. However, the results show that for the solar energy driven ORC system in this study, a recuperator should be configured.

Yang et al. [12] concluded that toluene has the best performance, which agrees well with our results in Table 4. However, the optimal system design derived from our work performs much better than the results reported by Yang et al. [12]. The reason is that our methodology optimizes the solar collector, the energy storage system and the ORC system simultaneously, and the optimal trade-off between the ORC system efficiency and the solar collector efficiency can be determined automatically by the PSO algorithm. Table 5 presents a detailed comparison between the results by Yang et al. [12] and the results obtained in this study.

In Yang et al. [12], the hot tank temperature is 375 °C, which is the highest temperature among all tested temperatures. However, for the basic ORC in our study, the optimal hot tank temperature is 368 °C, which is found by the optimizer. The cold tank temperature in our study is also lower than the reported value. For the basic ORC, the thermal efficiency is improved from 22.2% to 24.3%, while the system efficiency

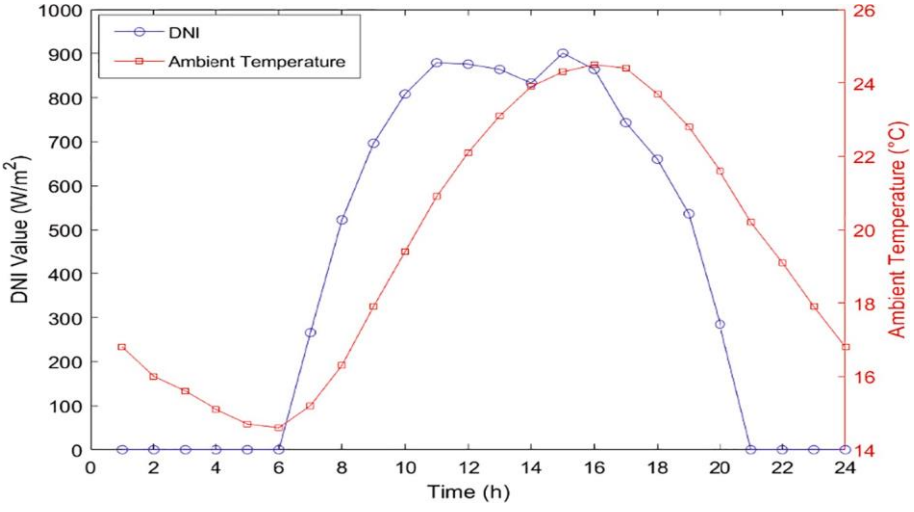

Fig. 4. The DNI and ambient temperatures for the given day [12].

Table 4
Optimal performance of basic and recuperative ORCs.

Working fluids	Basic ORC			Recuperative ORC		
	W_{net}(kW)	η_{ORC}(%)	η_{sys}(%)	W_{net}(kW)	η_{ORC}(%)	η_{sys}(%)
Toluene	70.53	24.3	17.4	100.5	36.3	24.8
Cyclohexane	61.89	22.4	15.3	97.91	35.5	24.1
HDSMO	44.73	15.2	11.0	93.33	33.9	23.0
n-Pentane	46.83	15.8	11.5	85.95	31.0	21.2
Benzene	69.57	23.9	17.2	97.68	35.1	24.1
n-Hexane	51.58	17.5	12.7	92.50	33.4	22.8
n-Pentane (supercritical)	–	–	–	95.31	34.5	23.5

is improved from 14.9% to 17.4%. For the recuperative ORC, the thermal efficiency is improved from 30.4% to 36.3%, while the system efficiency is improved from 17.9% to 24.8%. However, for the recuperative ORC in our work, the optimal hot tank temperature (399 °C) almost reaches the upper bound (400 °C). The fact that an optimization variable reaches a constraint (here an upper bound) indicates that the objective function could be improved with relaxed upper bound. As already mentioned, PTCs can effectively produce heat at temperatures between 50 and 400 °C. As a result, the upper bound for the hot tank temperature is set to 400 °C, and the heat transfer fluid used in this study (diphenyl oxide and biphenyl) can operate at this upper temperature. If another HTF applicable for a higher temperature range is used, the system performance could be improved further, however, such operation would need to be checked against the PTC behavior. The cold tank temperatures are quite different for the basic and recuperative ORC systems. The optimal cold tank temperature for the basic ORC is 57.6 °C, while it becomes 234.3 °C for the recuperative ORC. The temperature profiles in the evaporator for the basic and recuperative ORCs in our study are shown in Fig. 5. The flat range in working fluid curves for both basic ORC and recuperative ORC denotes a phase change. Since the optimal evaporation pressure is located at the upper bound (90% of the critical pressure of the working fluid), the flat range does not take up a big portion of the whole curve. It can be seen that the degree of superheating at the turbine inlet is very high for the recuperative ORC, thus the HTF and the toluene match well and the system efficiency is higher for the recuperative ORC (see Fig. 5).

The evaporation pressure in the basic ORC and recuperative ORC reaches the upper bound (37.12 bar) in both our study and the one by Yang et al. [12], which indicates that both the basic ORC and the recuperative ORC favor high evaporation pressure. In this study, the maximum evaporation pressure is set to 90% of the critical pressure to guarantee stable operation and reliable simulation results for the subcritical ORC. The upper bound can be relaxed if a supercritical ORC is considered, which will be discussed in detail later.

For the subcritical ORC without superheating, the pinch point between the working fluid and the heat source can be located either at the starting point of vaporization or at the starting point of preheating, also referred to as Vaporization Pinch Point (VPP) and Preheating Pinch Point (PPP) [31]. With reference to the results of the recuperative ORC with superheating as shown in Fig. 5, the pinch point can also be located at the superheating end, which can be termed Superheating Pinch Point (SPP). However, the degree of superheating in recuperative ORC can is around 100 °C as shown in Fig. 5. A large degree of superheating can increase the capital cost of the evaporator. To avoid too large degree of superheating, an easy way to handle this problem is to add a constraint to the model Since the HTF is a mixture, and the temperature profile is not a straight line, the pinch point can also be located in the preheating process as shown in Fig. 5 for the basic ORC. In both the basic and the recuperative ORCs, the phase change process exhibits a large temperature difference, which results in exergy losses.

Another considerable difference between the basic and recuperative ORCs is the cold tank temperature. As already mentioned with reference to Table 5, the cold tank temperatures are 57.6 °C and 234.3 °C for the basic and recuperative ORCs, respectively. This significant improvement in cold tank temperature can be explained as follows: The recuperator can preheat the working fluid to a higher temperature, which drives the cold tank temperature to a higher level. Therefore, both the ORC thermal efficiency and the system efficiency are improved with a recuperator.

4.2. *Impact of working fluids*

To investigate the effect of working fluids on system performance, other than the four working fluids studied by Yang et al. [12], two more working fluids (benzene and n-hexane) are investigated in this study. While toluene has the highest ORC thermal efficiency and system efficiency, one disadvantage is that its condensation pressure is less than the ambient pressure. This means that the turbine outlet stream is in vacuum, which can result in operational difficulties and safety issues for the system. Generally speaking, it is desired that the condensation pressure of the ORC is above ambient pressure. However, among all the investigated working fluids, only n-pentane can avoid vacuum condensation. The last column of Table 3 lists the saturation pressures at 50 °C. If the other working fluids also operate above ambient pressure, the condensation temperatures will be much higher than 50 °C, and the exact values are listed in the second last column of Table 3. If vacuum condensation is not allowed, the efficiency of the other working fluids will be significantly decreased. This means that n-pentane performs much better than the other working fluids if vacuum is not allowed in the ORC. In addition, for the recuperative ORC, the performance of n-pentane is not too far behind the other working fluids. From a practical point of view, n-pentane could therefore be the best choice.

Based on the results from this study, it can be concluded that the working fluids with higher critical temperature tend to have higher thermal efficiency, but the condensation pressure can be lower than the ambient pressure. Vacuum condensation will increase the operation

Table 5
Comparison with Yang et al. [12] using toluene as the working fluid.

	Cycle type	T_{hot}(°C)	T_{cold}(°C)	P_{eva}(bar)	T_{tur}^{inlet}(°C)	η_{orc}(%)	η_{sys}(%)
Yang et al. [12]	Basic ORC	375	71.7	37.12	311.5	22.2	14.9
	Recuperative	375	251.9	37.12	355.0	30.4	17.9
This work	Basic ORC	368	57.6	37.12	313.3	24.3	17.4
	Recuperative	399	234.3	37.12	395.5	36.3	24.8

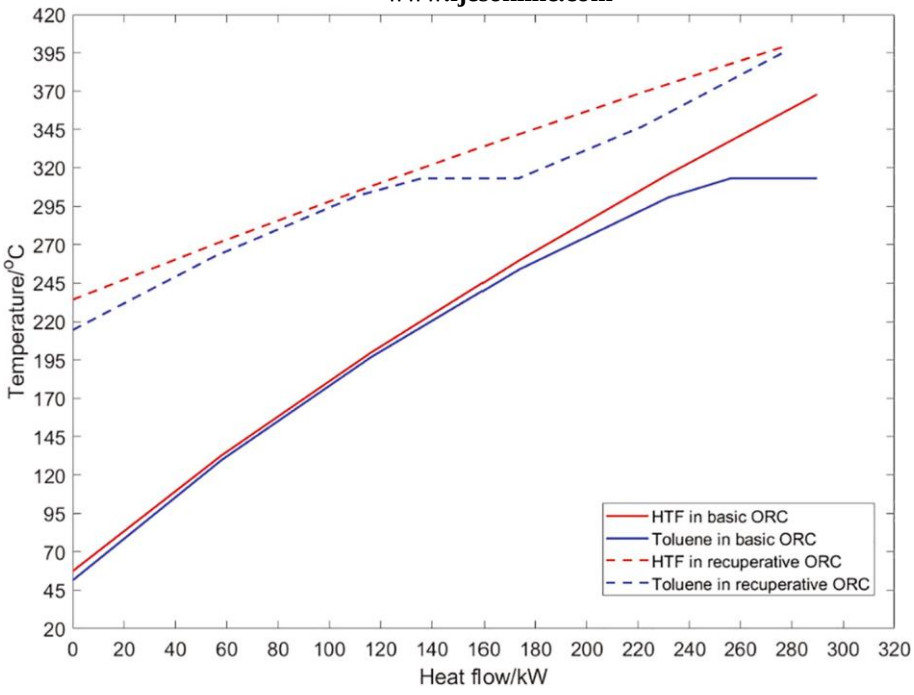

Fig. 5. Temperature profiles in the evaporator for the basic and recuperative ORC systems.

complexity, and there is a trade-off between thermal efficiency and operational complexity. The working fluids featuring both higher critical pressure and higher saturation pressure for the condensation temperature are desired for the ORC system. If this issue is considered, computer-aided molecular design techniques may discover more promising working fluids for the ORC.

4.3. Subcritical versus supercritical ORC

As already mentioned, the optimal evaporation pressure reaches the upper bound for both the basic and recuperative ORC, which indicates that the evaporation pressure could be a bottleneck in the system. To investigate the impact of the evaporation pressure on the system performance, the upper bound of the evaporator pressure is relaxed to supercritical pressures. With n-hexane as the working fluid, the upper bound of the evaporation pressure is set to 90% of the critical pressure (30.31 bar, see Table 3) for subcritical ORC and 100 bar for supercritical ORC respectively. When the upper bound of the evaporation pressure is less than the critical pressure, there is always phase change in the evaporator. In contrast, the ORC can be either subcritical or supercritical if the upper bound of the evaporation pressure is relaxed to 100 bar.

The last row in Table 4 lists the optimal results for the recuperative supercritical ORC with n-pentane as the working fluid. Compared with the subcritical ORC, the net power output is increased from 85.95 kW to 95.31 kW. The ORC thermal efficiency is improved by 11.3% (from 31.0% to 34.5%), and the system efficiency is improved by 10.8% (from 21.2% to 23.5%). Fig. 6 illustrates the temperature profiles in the recuperator and evaporator under both subcritical and supercritical

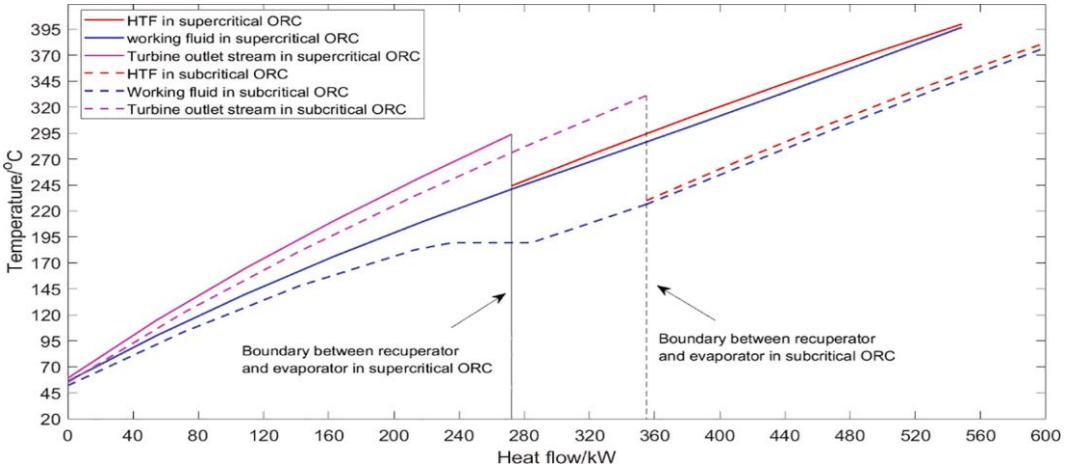

Fig. 6. Temperature profiles in the recuperator and evaporator under subcritical and supercritical conditions with n-pentane as the working fluid.

conditions. Interestingly, for the subcritical ORC, the phase change of n-pentane takes place in the recuperator, while the evaporator just superheats the working fluid. The phase change causes a flat range for the working fluid curve in the subcritical ORC. On the contrary, there is no such flat range for the working fluid curve in the supercritical ORC. The working fluid and the HTF match very well in the evaporator. The temperature profiles in the evaporator are almost the same for the subcritical and supercritical ORC systems, while the temperature profiles are quite different in the recuperator.

4.4. Optimal operation of the solar collectors

The optimal operation of this system refers to the control of the mass flowrate of the HTF to the solar collector. This is the only dynamic variable in the system, while other parts of the system should be in steady state. Only if the mass flowrate of the HTF is controlled properly, the system can be operated steadily at nominal design conditions. Once the cold and hot tank temperatures are determined, the mass flowrate of the HTF can be calculated by Eq. (5). Fig. 7 illustrates the optimal mass flowrate of the HTF in each time interval for a given day with toluene as the working fluid. The corresponding control measures can be taken to achieve the optimal operation of the integrated system. It is obvious that the mass flowrate of the HTF varies with the DNI value. For the recuperative ORC, the mass flowrate of the HTF is much higher than for the basic ORC. The mass flowrate of HTF in the recuperative ORC is 55.5% higher than that of the basic ORC, which indicates the tank size in the recuperative ORC should be at least 1.55 times of the tanks in the basic ORC. This can be attributed to the small temperature difference at the solar collector inlet and outlet in the recuperative ORC. The recuperative ORC outperforms the basic ORC in terms of ORC thermal efficiency and overall system efficiency. However, the basic ORC has the advantage of lower mass flowrate of HTF, which means the volumes of the storages tank can be smaller. If the volumes of the tanks become large, with a corresponding high capital cost, the HTF must be chosen carefully. An HTF with higher specific heat capacity will reduce the need for larger storage tanks. Also, other thermodynamic properties of the HTF should be considered in the selection process.

Fig. 7 also illustrates the solar collector efficiency variation with time. It is interesting that the solar collector efficiency in the basic ORC is higher than that in the recuperative ORC. This can be attributed to the smaller temperature difference between the average solar collector temperature and ambient temperature in the recuperative ORC. Unlike the mass flowrate of the HTF, the efficiency of the solar collector is quite stable. The efficiency is almost constant except for the time without solar radiation.

In summary, the system configuration, choice of working fluid and the operating conditions (subcritical vs. supercritical) exert great influence on the system performance. All these factors have to be taken into account simultaneously while designing such a solar driven PTC power plant. Although the analysis is conducted for given DNI values for one day, the proposed model can be applied to different days, months, and locations. The DNI values can be predicted from historical data, and a more robust system design can be obtained based on more comprehensive DNI values. Moreover, the ORC power station can also act as a peak shaving power plant, which means that the ORC only operates a few hours per day. The corresponding optimal system design and operation can be determined in the same way based on the model developed in this study. Only the number of operating hours needs to be changed in the model. In Eq. (7), the number of hours should be changed from 24 to a specific number. In Eq. (12), however, only the numerator needs to be changed (from 24 to a specific number), while the denominator remains the same, since it denotes the total solar energy in one day.

4.5. Recent developments and future directions

Recently, Eterafi et al. [32] also investigated the solar driven ORC system with stable output. Domestic hot water production is considered alone with the ORC system for power generation. The prominent role of thermal energy storage system is also examined. The solar collector is parabolic dish concentrator (PDC) instead of PTC used in our study. Aghaziarati and Aghdam [33] performed the thermoeconomic analysis of a solar energy driven combined system consisting of ORC, cascaded refrigeration and heating system. They also compared three different types of solar collectors (PTC, PDC and LFR). Therefore, many more different types of solar collectors should be investigate and compared in the future research. Also, the cogeneration system design could be an interesting direction since multi-products can enhance the opportunities for process integration. Last but not least, the stochastic and seasonal variation of long-term solar radiation and weather impacts on the assessment of solar energy capture and use should be addressed. In this regard, stochastic optimization for the design and selection of candidate

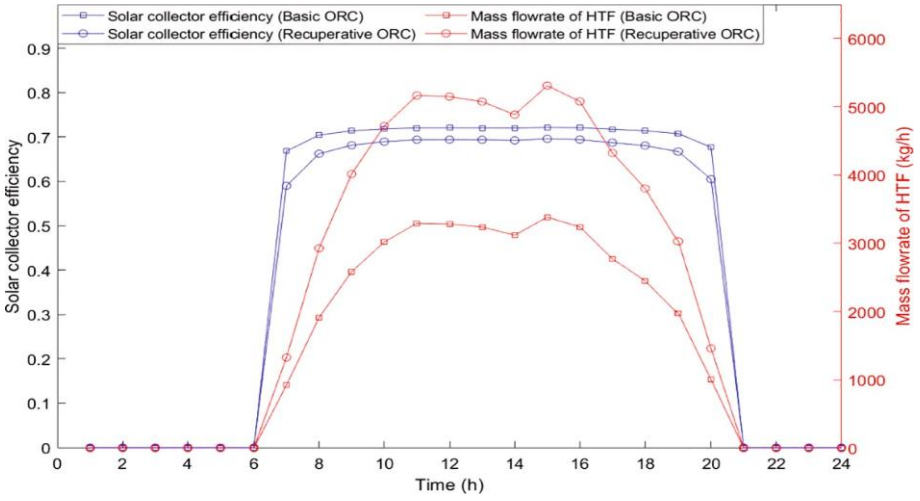

Fig. 7. Optimal HTF flowrate and solar collector efficiency for both basic and recuperative ORC with toluene as working fluid.

working fluids [34] under uncertainty [35] in the solar radiation will be investigated.

5. Conclusions

This study investigates the optimal design and operation of a solar energy driven ORC system with a parabolic trough collector and a two-tank sensible thermal energy storage system. The energy storage system and the ORC system have been optimized simultaneously to achieve the best performance of the total system. The power cycle system can reach a stable and continuous operation through a given day with the help of the two-tank energy storage system. The optimal trade-off between the solar collector efficiency and the power output of the ORC system has been determined by the proposed simulation-based optimization framework. The optimal flowrate of the heat transfer fluid during the whole day can be determined based on this model. The impact of the ORC system configuration (with or without recuperator), working fluid selection and the mode of operation (i.e. subcritical vs. supercritical) on the system performance is analyzed. The thermal efficiency of recuperative ORC is about 11.2–18.7% points higher than that of a basic ORC system, while the improvement in overall system efficiency is about 6.9–12% points higher. Toluene performs best among all the investigated working fluids ignoring the problems with vacuum condensation. Compared with the study by Yang et al. [35], the overall system performance is improved substantially. Our methodology can improve the ORC thermal efficiency from 22.2% (previously reported value) to 24.3%, while the system efficiency is improved from 14.9% (previously reported value) to 17.4% for basic ORC. For the recuperative ORC, the ORC thermal efficiency is improved from 30.4% to 36.3%, while the overall system efficiency is improved from 17.9% to 24.8%. Using n-pentane as working fluid, vacuum condensation can be avoided, and both subcritical and supercritical operations are investigated with n-pentane as the working fluid. The supercritical ORC with n-pentane as working fluid can improve the ORC thermal efficiency by 11.3% and the system efficiency by 10.8% compared with the subcritical ORC. In this study, only sensible thermal energy storage is considered, while latent thermal energy storage systems or combined latent and sensible thermal energy storage systems are also interesting options, which deserve thorough comparative research in future work.

CRediT authorship contribution statement

Haoshui Yu: Conceptualization, Supervision, Software, Formal analysis, Writing - original draft. **Henrik Helland:** Software, Methodology, Formal analysis, Validation. **Xingji Yu:** Software, Formal analysis, Writing - review & editing. **Truls Gundersen:** Conceptualization, Investigation, Writing - review & editing. **Gürkan Sin:** Investigation, Writing - review & editing.

Declaration of Competing Interest

The authors declare that they have no known competing financial interests or personal relationships that could have appeared to influence the work reported in this paper.

Acknowledgments

The authors gratefully acknowledge the financial support from MIT Energy Initiative CCUS Low Carbon Energy Center, H2020 Marie Skłodowska-Curie Actions-Individual Fellowships (891561) and the Research Council of Norway and user partners of HighEFF, an 8-year Research Centre under the FME-scheme (Centre for Environment-friendly Energy Research, 257632). We would also like to thank the authors of reference [12] for sharing the DNI and ambient temperature data with us.

References

[1] Patil VR, Biradar VI, Shreyas R, Garg P, Orosz MS, Thirumalai NC. Techno-economic comparison of solar Organic Rankine Cycle (ORC) and photovoltaic (PV) systems with energy storage. Renewable Energy 2017;113:1250–60.
[2] Kshirsagar AN, Garg P, Kumar P, Orosz MS, Vidyanagari P. Effect of temperature difference across ORC boiler on the thermal storage medium cost in a solar ORC. 3rd International Seminar on ORC Power Systems Brussels. 2015.
[3] Pelay U, Luo L, Fan Y, Stitou D, Rood M. Thermal energy storage systems for concentrated solar power plants. Renewable Sustainable Energy Rev 2017;79: 82–100.
[4] Kalogirou SA. Solar thermal collectors and applications. Prog Energy Combust Sci 2004;30(3):231–95.
[5] Casati E, Galli A, Colonna P. Thermal energy storage for solar-powered Organic Rankine Cycle engines. Sol Energy 2013;96:205–19.
[6] Yu H, Feng X, Wang Y, Biegler LT, Eason J. A systematic method to customize an efficient Organic Rankine Cycle (ORC) to recover waste heat in refineries. Appl Energy 2016;179:302–15.
[7] Yu H, Eason J, Biegler LT, Feng X. Process integration and superstructure optimization of Organic Rankine Cycles (ORCs) with heat exchanger network synthesis. Comput Chem Eng 2017;107:257–70.
[8] Mehrpooya M, Sharifzadeh MMM. A novel integration of oXy-fuel cycle, high temperature solar cycle and LNG cold recovery–energy and exergy analysis. Appl Therm Eng 2017;114:1090–104.
[9] Ahmadi MH, Mehrpooya M, Abbasi S, Pourfayaz F, Bruno JC. Thermo-economic analysis and multi-objective optimization of a transcritical CO2 power cycle driven by solar energy and LNG cold recovery. Therm Sci nd Eng Progress 2017;4:185–96.
[10] Cocco D, Serra F. Performance comparison of two-tank direct and thermocline thermal energy storage systems for 1 MWe class concentrating solar power plants. Energy 2015;81:526–36.
[11] Wang J, Yan Z, Zhao P, Dai Y. Off-design performance analysis of a solar-powered Organic Rankine Cycle. Energy Convers Manage 2014;80:150–7.
[12] Yang J, Li J, Yang Z, Duan Y. Thermodynamic analysis and optimization of a solar Organic Rankine Cycle operating with stable output. Energy Convers Manage 2019;187:459–71.
[13] Tzivanidis C, Bellos E, Antonopoulos KA. Energetic and financial investigation of a stand-alone solar-thermal Organic Rankine Cycle power plant. Energy Convers Manage 2016;126:421–33.
[14] Sharma A, Tyagi VV, Chen CR, Buddhi D. Review on thermal energy storage with phase change materials and applications. Renewable Sustainable Energy Rev 2009; 13(2):318–45.
[15]

Manfrida G, Secchi R, Stanczyk K. Modelling and simulation of phase change material latent heat storages applied to a solar-powered Organic Rankine Cycle.Appl Energy 2016;179:378–88.

[16] Chacartegui R, Vigna L, Becerra JA, Verda V. Analysis of two heat storage integrations for an Organic Rankine Cycle Parabolic trough solar power plant.Energy Convers Manage 2016;125:353–67.

[17] Blanco J, Alarcón D, Sánchez B, Malato S, Maldonado MI, Hublitz A, et al. Technical comparison of different solar-assisted heat supply systems for a multi- effect seawater distillation unit. In ISES Solar World Congress, Göteborg, Sweden, June2003. p. 14-9.

[18] Lang C, Lee B. Heat transfer fluid life time analysis of diphenyl oXide/biphenylgrades for concentrated solar power plants. Energy Procedia 2015;69:672–80.

[19] Lopez-Echeverry JS, Reif-Acherman S, Araujo-Lopez E. Peng-Robinson equation ofstate: 40 years through cubics. Fluid Phase Equilib 2017;447:39–71.

[20] Peng D-y, Robinson DB. A rigorous method for predicting the critical properties ofmulticomponent systems from an equation of state. AIChE J 1977;23(2):137–44.

[21] Yu H, Kim D, Gundersen T. A study of working fluids for Organic Rankine Cycles(ORCs) operating across and below ambient temperature to utilize Liquefied Natural Gas (LNG) cold energy. Energy 2019;167:730–9.

[22] Chen C-L, Chang F-Y, Chao T-H, Chen H-C, Lee J-Y. Heat-exchanger network synthesis involving Organic Rankine Cycle for waste heat recovery. Ind Eng ChemRes 2014;53(44):16924–36.

[23] Eberhart R, Kennedy J. A new optimizer using particle swarm theory. In: Proceedings of the siXth international symposium on micro machine and humanscience; 1995. p. 39–43.

[24] Javaloyes-Antón J, Ruiz-Femenia R, Caballero JA. Rigorous design of complex distillation columns using process simulators and the particle swarm optimizationalgorithm. Ind Eng Chem Res 2013;52(44):15621–34.

[25] Bai Q. Analysis of particle swarm optimization algorithm. Comput Inf Sci 2010;3(1):180.

[26] Jiang Y, Hu T, Huang C, Wu X. An improved particle swarm optimizationalgorithm. Appl Math Comput 2007;193(1):231–9.

[27] Garg P, Orosz MS. Economic optimization of Organic Rankine Cycle with pure fluids and miXtures for waste heat and solar applications using particle swarm optimization method. Energy Convers Manage 2018;165:649–68.

[28] Liu H, Zhang H, Yang F, Hou X, Yu F, Song S. Multi-objective optimization of fin-and-tube evaporator for a diesel engine-Organic Rankine Cycle (ORC) combined system using particle swarm optimization algorithm. Energy Convers Manag 2017;151(Supplement C):147–57.

[29] Pavão LV, Costa CBB, Ravagnani MASS. Heat EXchanger Network Synthesis without stream splits using parallelized and simplified simulated Annealing andParticle Swarm Optimization. Chem Eng Sci 2017;158:96–107.

[30] Yu H, Gundersen T, Feng X. Process integration of Organic Rankine Cycle (ORC) and heat pump for low temperature waste heat recovery. Energy 2018;160:330–40.